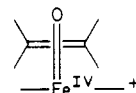


epoxidation reaction. That we find that it is necessary to involve a steric effect when using **NO** as the oxygen transfer agent suggests that in the case of oxygen transfer from **NO** to $(\text{Cl}_8\text{TPP})\text{Fe}^{\text{III}}\text{Cl}$, subsequent **DA** oxidation has very little steric requirement, and for this reason, **DA** oxidation competes most successfully with bulky arenes for the $[\text{Cl}_8\text{TPP}(\text{Cl})\text{Fe}^{\text{IV}}\text{O}]^+$ species. In Traylor's experiments, the steric effect would be of little importance because the $[\text{Cl}_8\text{TPP}(\text{Cl})\text{Fe}^{\text{IV}}\text{O}]^+$ is generated in the absence of all oxidizable substrates except for added alkene. When using either **NO** or pentafluoroiodosylbenzene, the rate-limiting step is oxygen transfer with substrate oxidation being much faster. In such a situation, the ratios of products formed are dependent upon the rate constants for the added substrate reacting with $[\text{Cl}_8\text{TPP}(\text{Cl})\text{Fe}^{\text{IV}}\text{O}]^+$. Examination of molecular models for $(\text{Cl}_8\text{TPP})\text{Fe}^{\text{IV}}\text{O}$

$\text{Fe}^{\text{III}}\text{Cl}$ and the X-ray data for $(\text{MeO})_8\text{TPP}\text{H}_2$ ¹¹ in conjunction with what would appear to be the most reasonable transition-state geometry for epoxidation¹² suggests that steric hindrance should be encountered when employing $(\text{Cl}_8\text{TPP})\text{Fe}^{\text{III}}\text{Cl}$ as the catalyst.



Acknowledgment. This work has been supported by a grant from The National Institutes of Health. We thank Prof. Teddy Traylor for allowing us to read his manuscript prior to its publication.

Registry No. TBPH, 732-26-3; TME, 563-79-1; $\text{Cl}_8(\text{TPP})\text{Fe}^{\text{III}}\text{Cl}$, 91042-27-2; *p*-cyano-*N,N*-dimethylaniline *N*-oxide, 62820-00-2; cyclohexene, 110-83-8.

(11) Gold, K. W.; Hodgson, D. J.; Gold, A.; Savrin, J. E.; Toney, G. E. *J. Chem. Soc., Chem. Commun.* **1985**, 563.

(12) (a) Collman, J. P.; Brauman, J. I.; Meunier, B.; Raybuck, S. A.; Kodadek, T. *Proc. Natl. Acad. Sci. U.S.A.* **1984**, *81*, 3245. (b) Groves, J. T.; Nemo, T. E. *J. Am. Chem. Soc.* **1983**, *105*, 5786.

Influence of Nitrogen Base Ligation and Hydrogen Bonding on the Rate Constants for Oxygen Transfer from Percarboxylic Acids and Alkyl Hydroperoxides to (*meso*-Tetraphenylporphinato)manganese(III) Chloride

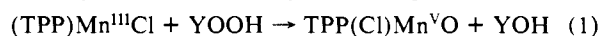
Lung-Chi Yuan and Thomas C. Bruice*

Contribution from the Department of Chemistry, University of California at Santa Barbara, Santa Barbara, California 93106. Received July 8, 1985

Abstract: Equilibrium constants for axial ligation of imidazole (ImH), *N*-methylimidazole (*N*-MeIm), 4'-(imidazo-1-yl)-acetophenone (NAcPhIm), 2,6-lutidine (2,6-Py), and 3,4-lutidine (3,4-Py) with (*meso*-tetraphenylporphinato)manganese chloride $(\text{TPP})\text{Mn}^{\text{III}}\text{Cl}$ have been determined. The rates of oxygen atom transfer from percarboxylic acids and alkyl hydroperoxides (YOOH) to the manganese(III) porphyrin in the presence of varying concentrations of the nitrogen bases were determined. For this purpose, 2,2-diphenyl-1-picrylhydrazine (DPPH) was employed as a trap for the generated higher valent oxo-manganese porphyrin species. From the equilibrium and kinetic data, there was then calculated the second-order rate constants for oxygen atom transfer from YOOH compounds to the species $(\text{TPP})\text{Mn}^{\text{III}}\text{Cl}$, $\text{TPP}(\text{Cl})\text{Mn}^{\text{III}}\text{N}$, and $\text{TPP}(\text{Cl})\text{Mn}^{\text{III}}\text{N}_2$ (where N = ImH, *N*-MeIm, and 3,4-Py). Only the percarboxylic acids exhibit measurable rate constants for oxygen transfer to $(\text{TPP})\text{Mn}^{\text{III}}\text{Cl}$, whereas alkyl hydroperoxides and percarboxylic acids transfer oxygen to the $\text{TPP}(\text{Cl})\text{Mn}^{\text{III}}\text{N}$ species. Of the species $\text{TPP}(\text{Cl})\text{Mn}^{\text{III}}\text{N}_2$, reaction with YOOH compounds is seen only when N is imidazole. This is attributed to an equilibrium of the unreactive bis axially ligated $\text{TPP}(\text{Cl})\text{Mn}^{\text{III}}(\text{ImH})_2$ with the reactive isomeric mono axial-ligated complex $\text{Cl}^- \cdots \text{H}-\text{Im} \cdots \text{H}-\text{Im} \cdots \text{Mn}^{\text{III}}\text{TPP}$. Nitrogen base ligation of $(\text{TPP})\text{Mn}^{\text{III}}\text{Cl}$ provides minimally a 10^3 increase in the rate constants for oxygen transfer in methylene chloride. Linear free-energy plots of the log of the second-order rate constants for oxygen transfer from YOOH vs. the $\text{p}K_a$ of YOH establish that β_{1g} for oxygen transfer in which heterolytic O-O bond scission is rate-determining is large and negative. The value of β_{1g} when oxygen transfer involves rate-determining homolytic O-O bond scission is small and negative.

Sligar and co-workers have successfully demonstrated the reconstitution of P-450_{CAM} with manganese protoporphyrin IX with retention of enzyme activity.¹ Model studies of P-450 and peroxidase have been focused on the investigations with manganese porphyrins, as well as iron porphyrins. A puzzling observation which has received much attention is that though manganese(III) porphyrin salts are good catalysts for oxidations with iododisylbenzene and percarboxylic acids, they are not reactive with alkyl hydroperoxides.²⁻⁵ We have recently shown that the lack of

reactivity of $(\text{TPP})\text{Mn}^{\text{III}}\text{Cl}$ with alkylhydroperoxides in benzonitrile is due to the very great sensitivity of the oxygen transfer to the acidity of the leaving group (YOH), eq 1.⁵ On the other



hand, the reactivity and stereoselectivity of manganese(III)

(2) Hill, C. L.; Smegal, J. A.; Henly, T. J. *J. Org. Chem.* **1983**, *48*, 3277.
(3) Mansuy, D.; Bartoli, J.-F.; Momenaueu, M. *Tetrahedron Lett.* **1982**, 23, 2781.

(4) Mansuy, D.; Bartoli, J.-F.; Chottard, J.-C.; Lange, M. *Angew. Chem., Int. Ed. Engl.* **1980**, *19*, 909.

(5) Yuan, L. C.; Bruice, T. C. *Inorg. Chem.* **1985**, *24*, 986.

(1) Gelb, M. H.; Toscano, W. A., Jr.; Sligar, S. G. *Proc. Natl. Acad. Sci. U.S.A.* **1982**, *79*, 5758.

Table I. Absorption Maxima and Association Constants for Various Amine-Ligated Manganese(III) Tetraphenylporphyrin Complexes^a

N-ligand	pK _a	K ₁ , M ⁻¹	β ₂ , M ⁻²	λ _{max} (TPP)Mn ^{III} (N-ligand) ₂ Cl
ImH	6.99 ^c 7.05 ^b	176 ± 20.5	62 900 ± 4600	472.0
<i>N</i> -Melm	6.95 ^b	96.3 ± 8.4	8530 ± 330	471.0
NAcPhIm		22.0	1000	
3,4-Py	6.48 ^c 6.61 ^d	10.5 ± 0.1	110.5 ± 7.0	479.0
2,6-Py	6.64 ^e	~0.33	nd ^e	

^a The measurements were carried out at 25 °C in CH₂Cl₂ (Aldrich, pre-treatment with Al₂O₃). ^b Data from: Jencks, W. P.; Regenstein, J. "Handbook of Biochemistry", 2nd ed.; CRC Press: New York, 1970, p J212. ^c From: Perrin, D. D. "Dissociation Constants of Organic bases in Aqueous Solution"; Butterworths: London, 1972. ^d From: Ikekawa, N.; Sato, Y.; Maeda, T. *Pharm. Bull.* **1954**, *2*, 205. ^e Too small to be determined.

porphyrin salts with alkylhydroperoxides and hypochlorites the manganese(III) porphyrin with the heterocyclic basis, *imidazole*⁶ and *pyridine*⁷ (and their derivatives). We report here (i) a rather detailed account of the influence of heterocyclic ligands on the rate of oxygen transfer from percarboxylic acids and hydroperoxides to manganese(III) tetraphenylporphyrin and (ii) a determination of the role of hydrogen bonding—in imidazole-ligated manganese(III) tetraphenylporphyrin—in the acceleration of the rate of oxygen transfer.

Experimental Section

Absorption spectra and spectral kinetic data were recorded with a Perkin-Elmer 553 fast-scanning UV-vis spectrophotometer. GC analyses were carried out with a Varian Model 3700 gas chromatograph equipped with a Hewlett-Packard 3392A integrator using a 25-m capillary column (Varian, WCOT, Vit. Silica). Rate constants were determined from plots of kinetic data by use of a Hewlett-Packard 982SA computer equipped with a 9864A digitizer and plotter.

Materials. Methylene chloride was purchased from Burdick & Jackson Laboratories, Inc. (99.9%, "Distilled in Glass" grade), or Aldrich (99+%, spectrophotometric grade; Gold Label). Chromatographic alumina (neutral, Type WN-3) from Sigma was baked in an oven at 120 °C in vacuo overnight before use. (*meso*-Tetraphenylporphinato)manganese(III) chloride ((TPP)Mn^{III}Cl) was prepared and purified according to a literature procedure.⁸ *p*-Nitroperbenzoic acid, *m*-chloroperbenzoic acid (MCPBA), cumyl hydroperoxide, and *tert*-butyl hydroperoxide (anhydrous, 3.0 M in toluene) were obtained from Aldrich and used without further purification. Phenylperacetic acid,⁹ perlauroic acid,¹⁰ diphenylhydroperoxyacetone,¹¹ methyl diphenylhydroperoxyacetate,¹² and triphenylmethyl hydroperoxide¹³ were prepared by known methods. The purity of all percarboxylic acids and hydroperoxides was determined by iodometric titration.¹⁴ 2,2-Diphenyl-1-picrylhydrazyl hydrate (DPP•) was available from Aldrich. 2,2-Diphenyl-1-picrylhydrazine (DPPH)

was prepared by sodium dithionite reduction of DPP• and recrystallized twice from CHCl₃/EtOH (2:3).¹⁵ 2,4,6-Tri-*tert*-butylphenol (TBPH) was available from Aldrich and purified by sublimation and recrystallization from 95% EtOH. Imidazole (ImH) and 4'-(imidazol-1-yl)-acetophenone (NAcPhIm) were available from Aldrich and recrystallized before use. *N*-Methylimidazole (*N*-Melm), 3,4-lutidine (3,4-Py), and 2,6-lutidine (2,6-Py) were available from Aldrich and purified by fractional distillation. The purities of *N*-methylimidazole, 3,4-lutidine, and 2,6-lutidine were analyzed by GC and determined to be >99.5%, ~100%, and 99.4%, respectively.

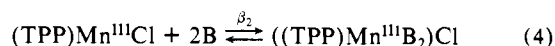
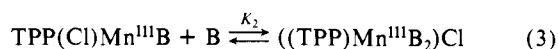
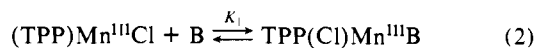
The determination of association constants (K_{ass}) was carried out by a method reported by Walker et al.¹⁶ All the spectra were recorded at 25 °C under aerobic conditions. The K₁ and β₂ values were determined by following the absorbance change of (TPP)Mn^{III} (~1.0 × 10⁻⁵ M) at 478 nm (Table I).

The determination of the percentage yield of phenylacetic acid, formed from the reaction of phenylperacetic acid with (TPP)Mn^{III}Cl in the presence of imidazole was determined by conversion to its methyl ester. In a 2-mL sealed bottle, 0.8 mL of a CH₂Cl₂ solution containing (TPP)Mn^{III}Cl (2.81 × 10⁻³ M), imidazole (4.15 × 10⁻³ M), and phenylperacetic acid (2.46 × 10⁻³ M) was allowed to stand at room temperature for 1 h when 0.30 mL of an ethereal solution of CH₂N₂ was added. GC analysis showed the yield of recovered ester, PhCH₂CO₂CH₃, to be 91.6 ± 1.7% based upon peracid employed.

The kinetics of oxygen transfer from percarboxylic acids and hydroperoxides to (TPP)Mn^{III} with a nitrogen-containing ligand (N-ligand) were carried out at 25 °C in dichloromethane. The concentration range of (TPP)Mn^{III}Cl and of percarboxylic acids or hydroperoxides (YOOH) was chosen on the basis of the reactivity of the YOOH species, and the concentration range of the N-ligand was chosen on the basis of the K_{ass}. The concentrations of DPPH, YOOH, and (TPP)Mn^{III}Cl were constant and in the order [DPPH] ≫ [YOOH] ≫ [(TPP)Mn^{III}Cl]. Kinetic studies were carried out over a 10-fold range of the concentrations of imidazole, *N*-methylimidazole, and 3,4-lutidine with each YOOH compound investigated. Typical conditions for the reaction of a nitrogen base ligated (TPP)Mn^{III}Cl with diphenylhydroperoxyacetone in the presence of DPPH are as follows: Methylene chloride solvent was passed through a short alumina column before use. A 2.80-mL aliquot of a methylene chloride solution containing (TPP)Mn^{III}Cl (1.25 × 10⁻⁵ M), imidazole (1.99 × 10⁻³ ~ 1.72 × 10⁻² M) and DPPH (8.80 × 10⁻³ M) was placed in the bottom part of a 1-cm Thunberg cuvette, and 0.2 mL of the appropriate dilution of a diphenylhydroperoxyacetone solution (1.51 × 10⁻⁴ M) was placed in the top part of the Thunberg cuvette. The reaction was initiated by mixing the two solutions and the reaction followed by monitoring the formation of DPP• at 600 nm. For slower reactions, such as the reaction of *t*-BuOOH and cumyl hydroperoxide with (TPP)Mn^{III}Cl in the presence of 3,4-lutidine and DPPH, higher concentrations of reactants were employed so that the reactions were carried out in 1.0-mm Thunberg cuvettes and followed at 700 nm.

Results

The association constants of imidazole, *N*-methylimidazole, 4'-(imidazol-1-yl)acetophenone, 3,4-lutidine, and 2,6-lutidine with (TPP)Mn^{III}Cl in methylene chloride (25 °C) were determined as described in the Experimental Section (eq 2 and 3). The



$$\beta_2 = K_1 K_2 \quad (5)$$

significant difference between the absorbance spectra of (TPP)Mn^{III}Cl and the bis complex of imidazole with (TPP)Mn^{III}Cl (i.e., ((TPP)Mn^{III}(ImH)₂)Cl) is found in the Soret band. A broadening shift from 478 nm (ε 9.31 × 10⁴) to 472 nm (ε 6.60 × 10⁴) accompanies the formation of the bis complex (Figure 1). The Soret band of the bis(3,4-lutidine) complex TPP(Cl)Mn^{III}(3,4-Py)₂ showed no shift but a broadening at 479 nm (ε 5.89 × 10⁴) (Figure 1). In Figure 2 are shown the typical spectral changes which take place in the Soret band region when imidazole is added to (TPP)Mn^{III}Cl. Two isosbestic points at 408 and 471 nm were ob-

(15) Traylor, T. G.; Lee, W. A.; Stynes, D. V. *Tetrahedron* **1984**, *40*, 553.

(16) Walker, F. A.; Lo, M.-W.; Ree, M. T. *J. Am. Chem. Soc.* **1976**, *98*, 5552.

(6) (a) Collman, J. P.; Brauman, J. I.; Meunier, B.; Hayashi, T.; Kodadek, T.; Raybuck, S. A. *J. Am. Chem. Soc.* **1985**, *107*, 2000. (b) Collman, J. P.; Brauman, J. I.; Meunier, B.; Raybuck, S. A.; Kodadek, T. *Proc. Natl. Acad. Sci. U.S.A.* **1984**, *81*, 3245. (c) Collman, J. P.; Kodadek, T.; Raybuck, S. A.; Meunier, B. *Ibid.* **1983**, *80*, 7039. (d) Mansuy, D.; Battioni, P.; Renaud, J.-P. *J. Chem. Soc., Chem. Commun.* **1984**, 1255.

(7) (a) Guilmet, E.; Meunier, B. *Nouv. J. Chim.* **1982**, *6*, 511. (b) Meunier, B.; Guilmet, E.; Carvalho, M.-E. D.; Poilblanc, R. *J. Am. Chem. Soc.* **1984**, *106*, 6668. (c) Razenberg, J. A. S. J.; Nolte, R. J. M.; Drenth, W. *Tetrahedron Lett.* **1984**, *25*, 789.

(8) Alder, A. D.; Longo, F. R.; Kampas, F.; Kim, J. J. *Inorg. Nucl. Chem.* **1970**, *32*, 2443.

(9) (a) McDonald, R. M.; Stepl, R. M.; Dorsey, J. E. *Org. Synth.* **1970**, *50*, 15. (b) White, R. E.; Sliagar, S. G.; Coon, M. J. *J. Biol. Chem.* **1980**, *255*, 11 108.

(10) Parker, W. E.; Ricciuti, C.; Ogg, C. L.; Swern, D. *J. Am. Chem. Soc.* **1955**, *77*, 4037.

(11) Seleksion, J. J.; Watt, D. S. *J. Org. Chem.* **1975**, *40*, 267.

(12) Avramoff, M.; Sprinzak, Y. *J. Am. Chem. Soc.* **1958**, *80*, 5433; **1963**, *85*, 1655.

(13) Yablokov, V. A. *Chem. Abst.* **1963**, *59*, 1515a.

(14) Johnson, R. M.; Siddiqui, I. W. "The Determination of Organic Peroxides"; Pergamon Press: New York, 1970; pp 15-29.

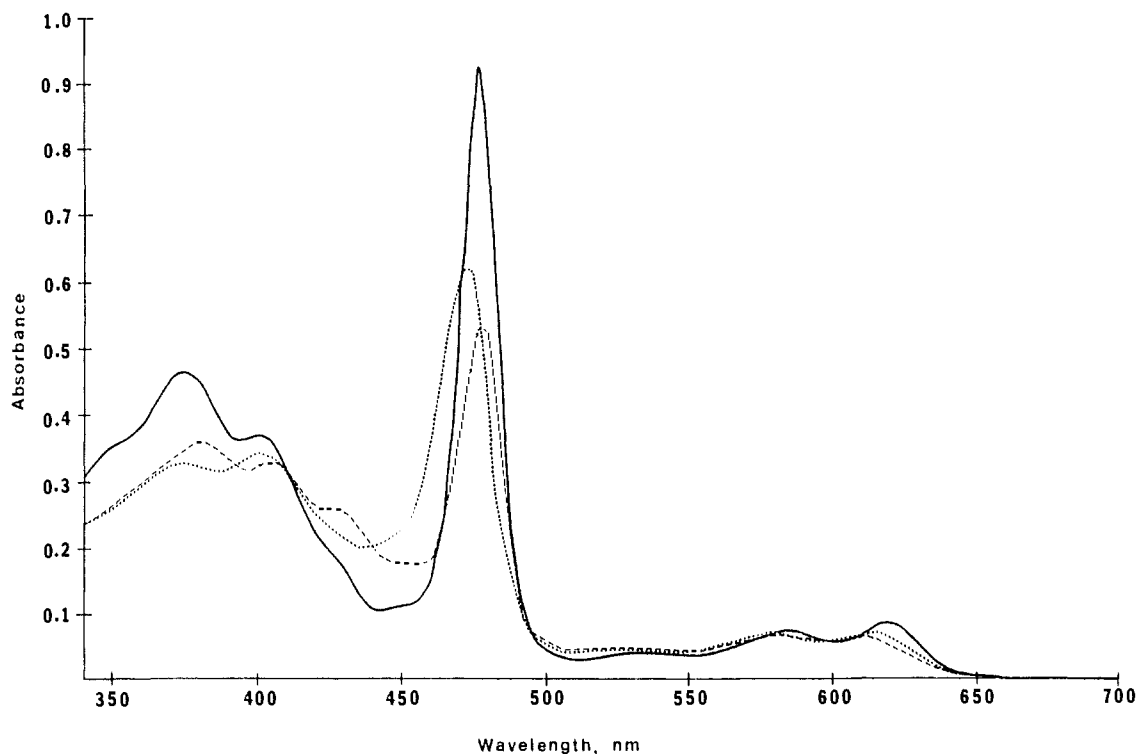


Figure 1. Visible spectra of (TPP)Mn^{III}Cl (1.49×10^{-5} M) (—), TPP(Cl)Mn^{III}(3,4-Py)₂ (1.35×10^{-5} M) (---), and TPP(Cl)Mn^{III}(ImH)₂ (1.39×10^{-5} M) (···) in CH₂Cl₂ at 25 °C.

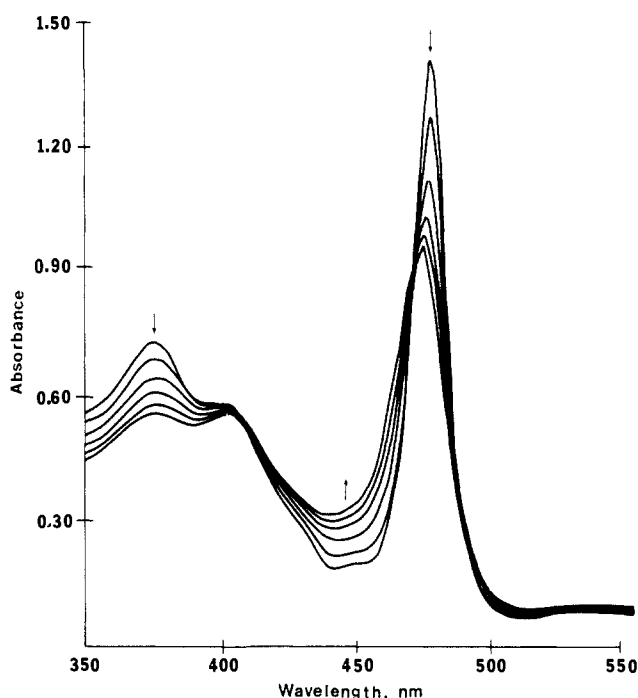


Figure 2. Visible spectra changes observed upon addition of imidazole to (TPP)Mn^{III}Cl (1.49×10^{-5} M) in CH₂Cl₂ at 25 °C.

served. The association constants, K_1 and β_2 , were calculated from absorbance data taken at 478 nm. The estimated K_1 , β_2 , and λ_{\max} of the Soret band of TPP(Cl)Mn^{III}(N-ligand)₂ are listed in Table I. The measurement of the association constants with 4'-(imidazol-1-yl)acetophenone was carried out by subtracting the absorbance contribution of 4'-(imidazol-1-yl)acetophenone from the observed absorbance at 478 nm for each determination. Due to the weak binding of 2,6-lutidine to (TPP)Mn^{III}Cl, the spectrum of (TPP)Mn^{III}(2,6-Py)₂Cl could not be determined. Therefore, the calculation of K_1 was based on the assumption that the spectrum of (TPP)Mn^{III}(2,6-Py)₂Cl is identical with the spectrum of (TPP)Mn^{III}(3,4-Py)₂Cl.

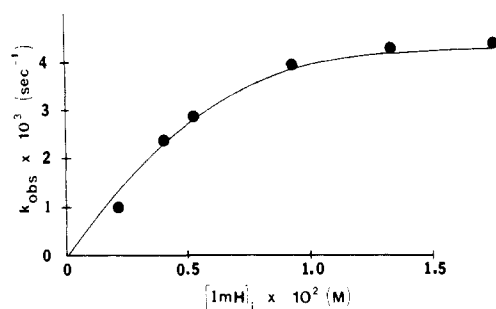


Figure 3. Plot of k_{obsd} vs. the concentration of the imidazole concentration for the reaction of (TPP)Mn^{III}Cl (1.03×10^{-5} M) with Ph₂C(CN)OOH (1.08×10^{-4} M) in the presence of DPPH (4.07×10^{-3} M) in CH₂Cl₂ at 25 °C.

Reaction of Diphenylhydroperoxyacetonitrile with (TPP)Mn^{III} Ligated to Imidazole. It has been determined that oxygen transfer from hydrogen peroxide and alkyl hydroperoxides to (TPP)Mn^{III}Cl is much slower than seen with (TPP)Cr^{III}Cl, (TPP)Fe^{III}Cl, and (TPP)Co^{III}Cl.^{2,5} Of the various alkyl hydroperoxides (YOOH) examined, diphenylhydroperoxyacetonitrile is the most reactive since it yields the most acidic leaving group (YOH). However, no apparent reaction was observed between this hydroperoxide and (TPP)Mn^{III}Cl in methylene chloride. Addition of imidazole to a reaction mixture composed to (TPP)Mn^{III}Cl (1.25×10^{-5} M) and diphenylhydroperoxyacetonitrile (1.51×10^{-4} M) containing the trapping agent DPPH (8.80×10^{-3} M) establishes that imidazole ligation results in the formation of DPP• (600 nm). Further, the rate of the reaction was found to be dependent on the concentration ($1.99 \times 10^{-3} \sim 1.72 \times 10^{-2}$ M) of imidazole employed (Figure 3) but independent of the concentration of DPPH within the range of concentrations employed (Table 11). As an example, no apparent difference of k_{obsd} was observed for the oxygen transfer from diphenylhydroperoxyacetonitrile (1.5×10^{-4} M) to (TPP)Mn^{III}Cl (1.25×10^{-5} M) in the presence of imidazole (1.99×10^{-3} M) with the range of DPPH concentrations of $4.05 \times 10^{-3} \sim 2.02 \times 10^{-2}$ M. The average yield of DPP• was $87 \pm 8\%$. The rate of formation of DPP• was also independent of [Ph₂C(CN)OOH]_i. As seen in Figure 4, values of k_{obsd} are

Table II. Independence on the Concentration of DPPH^a

DPPH, M	k_{obsd} , s ⁻¹
4.05×10^{-3}	1.05×10^{-3}
1.01×10^{-2}	1.16×10^{-3}
1.62×10^{-2}	1.13×10^{-3}
2.02×10^{-2}	1.01×10^{-3}

^a The initial concentrations of (TPP)Mn^{III}Cl, Ph₂C(CN)OOH, and imidazole were 1.25×10^{-5} , 1.51×10^{-4} , and 1.99×10^{-3} M, respectively (in CH₂Cl₂, 25 °C).

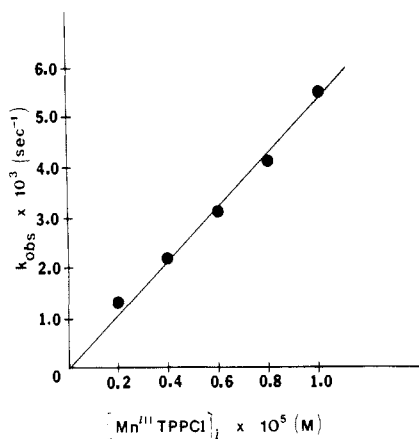
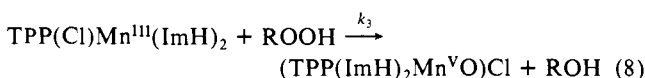
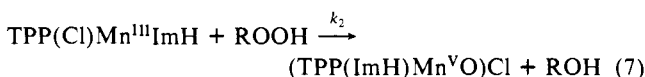
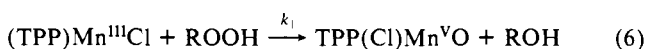


Figure 4. Plots of k_{obsd} as a function of (TPP)Mn^{III}Cl concentration when [Ph₂C(CN)OOH] = 1.05×10^{-4} M, [imidazole] = 1.76×10^{-2} M, and [DPPH] = 4.17×10^{-3} M (in CH₂Cl₂ at 25 °C).

linearly dependent upon [(TPP)Mn^{III}Cl]_i. Therefore, the rate of the oxygen-transfer reaction is only dependent upon the initial concentrations of (TPP)Mn^{III}Cl and imidazole. The appearance of DPP• followed first-order kinetics for 6~7 half-lives at 25 °C in methylene chloride. Within the concentration range of imidazole used, the manganese(III) tetraphenylporphyrin is partitioned between (TPP)Mn^{III}Cl, TPP(Cl)Mn^{III}ImH, and (TPP)Mn^{III}(ImH)₂Cl. The concentrations of these three species in any given reaction solution could be easily calculated from known initial concentrations of added reagents by use of the values of K_1 and β_2 (Table I). The dependence of k_{obsd} upon [imidazole]_i was analyzed by assumption of the reactions of eq 6–8 where k_1 , k_2 , and k_3 are the rate constants of oxygen transfer from diphenylhydroperoxyacetonitrile (ROOH) to (TPP)Mn^{III}Cl, TPP(Cl)Mn^{III}ImH, and (TPP)Mn^{III}(ImH)₂Cl, respectively. The pseu-



do-first-order rate constants (k_{obsd}) are the sum of k_1 [(TPP)Mn^{III}Cl], k_2 [TPP(Cl)Mn^{III}ImH], and k_3 [(TPP)Mn^{III}(ImH)₂Cl] as shown in eq 9. From eq 2 and 4, eq 9 can be rewritten as shown in eq 10. Since $k_{\text{obsd}} \gg k_1[(\text{TPP})\text{Mn}^{\text{III}}\text{Cl}]_i$ and $[\text{ImH}]_i \gg$

$$k_{\text{obsd}} = k_1[(\text{TPP})\text{Mn}^{\text{III}}\text{Cl}]_i + k_2[\text{TPP(Cl)Mn}^{\text{III}}\text{ImH}]_i + k_3[(\text{TPP})\text{Mn}^{\text{III}}(\text{ImH})_2\text{Cl}] \quad (9)$$

$$k_{\text{obsd}} = k_1[(\text{TPP})\text{Mn}^{\text{III}}\text{Cl}]_i + k_2K_1[(\text{TPP})\text{Mn}^{\text{III}}\text{Cl}]_i[\text{ImH}]_i + k_3\beta_2[(\text{TPP})\text{Mn}^{\text{III}}\text{Cl}]_i[\text{ImH}]_i^2 \quad (10)$$

$$\frac{k_{\text{obsd}}}{[(\text{TPP})\text{Mn}^{\text{III}}\text{Cl}]_i[\text{ImH}]_i} = k_2K_1 + k_3\beta_2[\text{ImH}]_i \quad (11)$$

[(TPP)Mn^{III}Cl]_i, eq 10 can be simplified to eq 11. Plots of $k_{\text{obsd}}/[(\text{TPP})\text{Mn}^{\text{III}}\text{Cl}]_i[\text{ImH}]_i$ vs. [ImH]_i are linear with intercepts equal to k_2K_1 and slopes equal to $k_3\beta_2$ (Figure 5). The rate constants for oxygen transfer, k_2 and k_3 , from diphenylhydro-

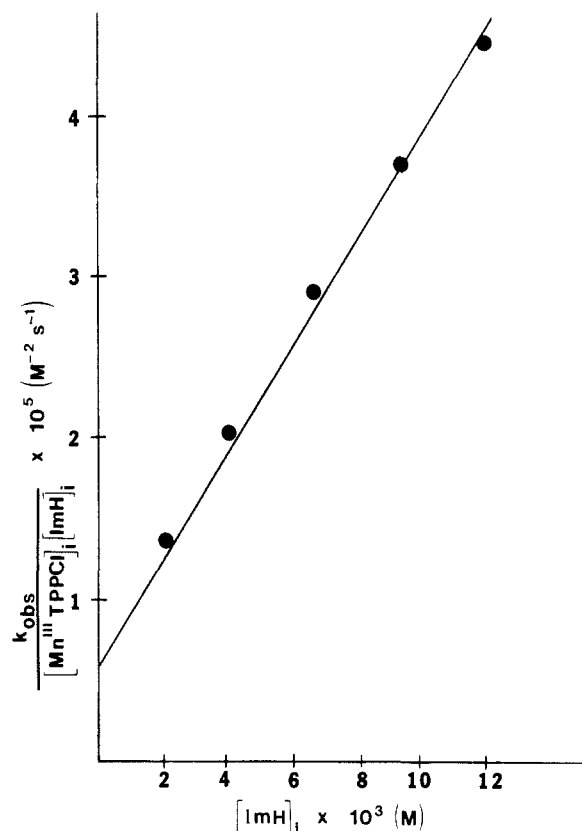


Figure 5. Method of analysis of $k_{\text{obsd}}/[(\text{TPP})\text{Mn}^{\text{III}}\text{Cl}]_i[\text{ImH}]_i$ vs. [ImH]_i data for the oxygen transfer from Ph₂C(CN)OOH (1.51×10^{-4}) to (TPP)Mn^{III}Cl (1.25×10^{-5} M) with imidazole (1.99×10^{-3} ~ 1.72×10^{-2} M) as the ligand.

peroxyacetonitrile to TPP(Cl)Mn^{III}ImH and (TPP)Mn^{III}(ImH)₂Cl were determined to be 335 and 522 M⁻¹ s⁻¹, respectively (eq 12 and 13).

$$k_2 = \text{intercept}/K_1 \quad (12)$$

$$k_3 = \text{slope}/\beta_2 \quad (13)$$

The influence of *N*-methylimidazole (*N*-MeIm) ligation to (TPP)Mn^{III} on the rate of oxygen transfer from diphenylhydroperoxyacetonitrile has been examined. The concentration of reagents employed were diphenylhydroperoxy acetonitrile, 1.33×10^{-4} M, (TPP)Mn^{III}Cl, 8.70×10^{-6} M, and DPPH, 5.25×10^{-3} M, while the concentration of *N*-MeIm was varied from 3.67×10^{-3} to 2.57×10^{-2} M. About 10% of the total change in A_{600} occurred rapidly on initiation of the reaction followed by a slower increase in A_{600} to the completion of the reaction. The two processes were dissected by fitting the plots of A_{600} vs. time to the rate equation for two sequential first-order reactions. The small burst in formation of DPP• was independent of [N-MeIm]_i and associated with a rate constant of $(7.64 \pm 0.78) \times 10^{-3}$ s⁻¹. The first-order rate constants for the slower and major portion of the change in A_{600} were dependent upon [N-MeIm]_i. The yield of DPP• varied from 75 to 40% and was inversely dependent upon [N-MeIm]_i. Apparently *N*-MeIm, or an impurity in the base, competes with DPPH for the higher valent oxo-manganese porphyrin species or reacts with DPP•. Formaldehyde could not be detected as a product in the reaction. This establishes dealkylation of *N*-MeIm as unlikely. From a knowledge of K_1 , β_2 , [(TPP)Mn^{III}Cl]_i, and [N-MeIm]_i, the concentration of (TPP)Mn^{III}Cl, which did not change its chloride ligand to *N*-MeIm, can be calculated. From eq 11, $k_{\text{obsd}}/[(\text{TPP})\text{Mn}^{\text{III}}\text{Cl}]_i[\text{N-MeIm}]_i$ was plotted vs. [N-MeIm]_i. The linear plot provided the intercept = 2.44×10^4 M⁻² s⁻¹ and slope = 0 (Figure 6). From the intercept, there was calculated (eq 12) the value of k_2 as 207 M⁻¹ s⁻¹. The rate constant k_2 pertains to the second-order rate constant for oxygen donation from Ph₂C(CN)OOH to (TPP)Mn^{III}(*N*-

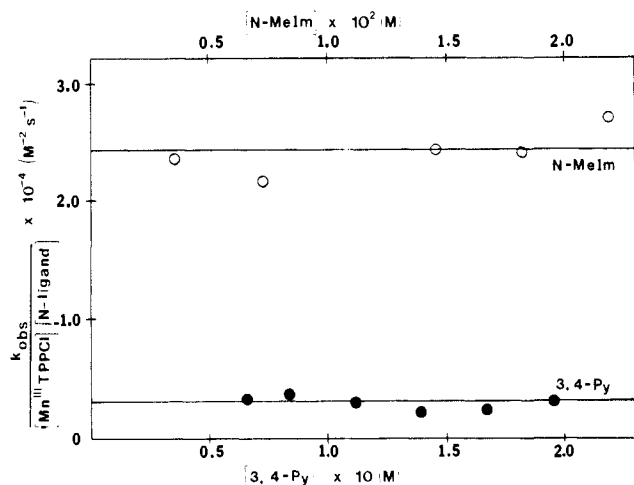


Figure 6. Plots of $k_{\text{obsd}}/[(\text{TPP})\text{Mn}^{\text{III}}\text{Cl}][\text{N-ligand}]_i$ vs. $[\text{3,4-Py}]_i$ (●) and $[\text{N-MeIm}]_i$ (○) for the oxygen transfer from $\text{Ph}_2\text{C}(\text{CN})\text{OOH}$ to $(\text{TPP})\text{Mn}^{\text{III}}\text{Cl}$ with 3,4-lutidine and *N*-methylimidazole as the N-ligand.

MeIm)Cl. Since the slope of Figure 6 equals zero, k_3 is unimportant and we may assume that any reaction occurring between $\text{Ph}_2\text{C}(\text{CN})\text{OOH}$ and $(\text{TPP})\text{Mn}^{\text{III}}(\text{N-MeIm})_2\text{Cl}$ is undetectable.

Similar kinetic behavior was observed in the reaction of *t*-BuOOH with $(\text{TPP})\text{Mn}^{\text{III}}\text{Cl}$ in the presence of varying concentrations of *N*-MeIm when monitored by the oxidation of DPPH to DPP. The rate constants k_2 and k_3 were determined as before and found to be 0.62 s^{-1} and 0. Thus, oxygen transfer from *t*-BuOOH to manganese(III) tetraphenylporphyrin does not occur at a measurable rate when Cl⁻ is the axial ligand but does so readily with *N*-MeIm as the axial ligand.

3,4-Lutidine-Manganese(III) Porphyrin Complex. Compared to imidazole and *N*-methylimidazole, pyridines are weak ligands to manganese porphyrins as shown by inspection of Table I. A kinetic study of oxygen transfer from diphenylhydroperoxyacetonitrile ($1.13 \times 10^{-4} \text{ M}$) to $(\text{TPP})\text{Mn}^{\text{III}}\text{Cl}$ ($1.03 \times 10^{-5} \text{ M}$) in the presence of 3,4-lutidine (3,4-Py) ($3.34 \times 10^{-2} \sim 2.34 \times 10^{-1} \text{ M}$) and DPPH ($4.28 \times 10^{-3} \text{ M}$) was also carried out in methylene chloride at 25 °C. All the reactions followed first-order kinetics for 6~7 half-lives. Plots of $k_{\text{obsd}}/[(\text{TPP})\text{Mn}^{\text{III}}\text{Cl}][\text{3,4-Py}]_i$ vs. $[\text{3,4-Py}]_i$ (Figure 6) where of zero slope and of intercept equal to $3150 \text{ M}^{-2} \text{ s}^{-1}$. The rate constant k_2 for oxygen transfer from diphenylhydroperoxyacetonitrile to $(\text{TPP})\text{Mn}^{\text{III}}(\text{3,4-Py})\text{Cl}$ was calculated (eq 12) to be $298 \text{ M}^{-1} \text{ s}^{-1}$. It can be concluded that there is no measurable rate of oxygen transfer from diphenylhydroperoxyacetonitrile to $(\text{TPP})\text{Mn}^{\text{III}}(\text{3,4-Py})_2\text{Cl}$. According to the same method, the oxygen transfer from *t*-BuOOH was also studied. Under the condition $[\text{DPPH}] = 5.92 \times 10^{-2} \text{ M} \gg [\text{t-BuOOH}] = 2.37 \times 10^{-3} \text{ M} \gg [(\text{TPP})\text{Mn}^{\text{III}}\text{Cl}] = 1.67 \times 10^{-4} \text{ M}$, the reactions were followed by the formation of DPP• at 700 nm in a concentration range of 3,4-lutidine between 1.06×10^{-1} and $3.90 \times 10^{-2} \text{ M}$. As before, a plot of $k_{\text{obsd}}/[(\text{TPP})\text{Mn}^{\text{III}}\text{Cl}][\text{3,4-Py}]_i$ vs. $[\text{3,4-Py}]_i$ provided a positive intercept ($7.5 \text{ M}^{-2} \text{ s}^{-1}$) and a zero slope. From the intercept, there was calculated a value for k_2 of $0.72 \text{ M}^{-1} \text{ s}^{-1}$ and from the slope a k_3 value of zero. The rate constants for oxygen transfer from diphenylhydroperoxyacetonitrile and *t*-BuOOH when employing $(\text{TPP})\text{Mn}^{\text{III}}\text{Cl}$ in the presence of various amines are summarized in Table III.

Oxygen transfers from a number of percarboxylic acids and hydroperoxides to $(\text{TPP})\text{Mn}^{\text{III}}\text{ImH}$ and $(\text{TPP})\text{Mn}^{\text{III}}(\text{ImH})_2$ were studied in methylene chloride at 25 °C by following the formation of DPP• at 600 nm. The YOOH species employed were *p*-nitroperbenzoic acid, *m*-chloroperbenzoic acid (MCPBA), phenylperacetic acid, perlauric acid, diphenylhydroperoxyacetonitrile, methyl diphenylhydroperoxyacetate, cumyl hydroperoxide, and *t*-BuOOH. Reactions were carried out such that $[\text{DPPH}]_i \gg [\text{YOOH}]_i \gg [(\text{TPP})\text{Mn}^{\text{III}}\text{Cl}]_i$, and the concentration of imidazole was varied over a 10-fold range. All the reactions followed pseudo-first-order kinetics and k_{obsd} was found to be dependent upon $[\text{ImH}]_i$. The term $k_{\text{obsd}}/[(\text{TPP})\text{Mn}^{\text{III}}\text{Cl}][\text{ImH}]_i$ was

Table III. Rate Constants of Oxygen Transfer from Diphenylhydroperoxyacetonitrile and *tert*-Butyl Hydroperoxide Mononitrogen Base Ligated (k_2) and Bis Nitrogen Base Ligated (k_3) $(\text{TPP})\text{Mn}^{\text{III}}\text{Cl}$ when Nitrogen Bases are Imidazole, *N*-Methylimidazole, and 3,4-Lutidine

ligand	hydroperoxide	$k_2, \text{M}^{-1} \text{s}^{-1}$	$k_3, \text{M}^{-1} \text{s}^{-1}$
imidazole	$\text{Ph}_2\text{C}(\text{CN})\text{OOH}$	335	522
	$(\text{CH}_3)_3\text{COOH}$	0.37	1.3
<i>N</i> -methylimidazole	$\text{Ph}_2\text{C}(\text{CN})\text{OOH}$	207	0
	$(\text{CH}_3)_3\text{COOH}$	0.63	0
3,4-lutidine	$\text{Ph}_2\text{C}(\text{CN})\text{OOH}$	298	0
	$(\text{CH}_3)_3\text{COOH}$	0.72	0

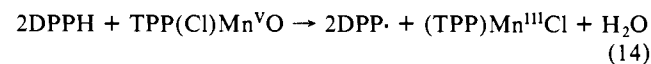
Table IV. k_2 and k_3 Values of Oxygen Transfer from a Series of Monooxygen Donors to $(\text{TPP})\text{Mn}^{\text{III}}\text{ImH}$ or $(\text{TPP})\text{Mn}^{\text{III}}(\text{ImH})_2\text{Cl}$ (in CH_2Cl_2 , 25 °C)

monooxygen donors	$\text{p}K_a$	$k_2, \text{M}^{-1} \text{s}^{-1}$	$k_3, \text{M}^{-1} \text{s}^{-1}$	yield of DPP• (%)
<i>p</i> -NO ₂ -Ph-CO ₂ H	3.44	7.78×10^5	2.76×10^6	52.6
MCPBA	3.83	3.16×10^5	1.31×10^6	76.9
$\text{PhCH}_2\text{CO}_2\text{H}$	4.31	1.76×10^5	6.98×10^5	69.2
$\text{CH}_3(\text{CH}_2)_{10}\text{CO}_2\text{H}$	4.86	3.41×10^4	1.24×10^5	53.9
$\text{Ph}_2\text{C}(\text{CN})\text{OOH}$	9.10	3.35×10^2	5.22×10^2	86.7
$\text{Ph}_2\text{C}(\text{CO}_2\text{Me})\text{OOH}$	11.07	5.00	10.30×10^1	12.0
$\text{PhC}(\text{CH}_3)_2\text{OOH}$	15.50	3.30×10^{-1}	3.70	57.0
$(\text{CH}_3)_3\text{COOH}$	16.73	3.70×10^{-1}	1.33	53.2

plotted vs. $[\text{ImH}]_i$ and the intercepts and slopes of the resultant linear plots were divided by K_1 and β_2 , respectively, to obtain k_2 and k_3 values. Values of k_2 and k_3 represent the rate constants for oxygen transfer from an oxidant to $(\text{TPP})\text{Mn}^{\text{III}}\text{ImH}$ and $(\text{TPP})\text{Mn}^{\text{III}}(\text{ImH})_2\text{Cl}$, respectively (Table IV).

Discussion

The object of the present investigation has been to determine the influence of nitrogen base ligation on the rate of oxygen transfer from percarboxylic acids and alkyl hydroperoxides (YOOH) to the metal center of (*meso*-tetraphenylporphinato)-manganese(III) chloride to generate nitrogen base ligated $(\text{TPP})\text{Mn}^{\text{III}}\text{Cl}$ (eq 1). 2,4,6-Tri-*tert*-butylphenol (TBPH) has previously been shown to be a suitable trapping agent for the iron-oxo porphyrin π -cation radical generated from $(\text{TPP})\text{Fe}^{\text{III}}\text{Cl}$ on its reaction with YOOH species (CH_3OH solvent)^{15,17,18} or with *p*-cyano-*N,N*-dimethylaniline *N*-oxide (CH_2Cl_2 solvent).¹⁹ However, we found the trapping efficiency of TBPH (0.1–0.2 M) to be insufficient for our purposes. A trapping agent of choice has been found in 2,2-diphenyl-1-picrylhydrazine (DPPH). DPPH has been employed in this study to trap the unstable and strongly oxidizing $(\text{TPP})\text{Mn}^{\text{III}}\text{Cl}$ product (eq 14). We chose DPPH as



the trapping agent for all the measurements of rate constants in this study because (i) DPP• has a high absorbance in the visible region ($>500 \text{ nm}$), (ii) the redox potential of DPPH at 770 mV is lower than that for TBPH at 984 mV,¹⁵ and (iii) DPP• is stable in air so that rate constants for oxygen transfer can be measured under either aerobic or anaerobic conditions.

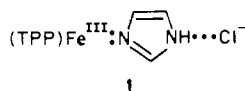
Before discussing the dynamics of oxygen transfer from YOOH species to nitrogen-ligated manganese(III) tetraphenylporphyrin, it is appropriate to consider the equilibrium complexation involved in the generation of the reactive species. It is a general finding with iron(III) porphyrins that the bis imidazole complexes are favored over the monoimidazole complexes. Thus, for $(\text{TPP})\text{Fe}^{\text{III}}\text{Cl}$, the equilibrium constant K_2 is larger than 10^6 M^{-1} while K_1 was not measurable.¹⁶ The only exception has been reported

(17) Lee, W. A.; Bruce, T. C. *J. Am. Chem. Soc.* **1985**, *107*, 513.

(18) Traylor, T. G.; Lee, W. A.; Stynes, D. V. *J. Am. Chem. Soc.* **1984**, *106*, 755.

(19) Dicken, C. M.; Lu, F. L.; Nee, M. W.; Bruce, T. C. *J. Am. Chem. Soc.*, in press.

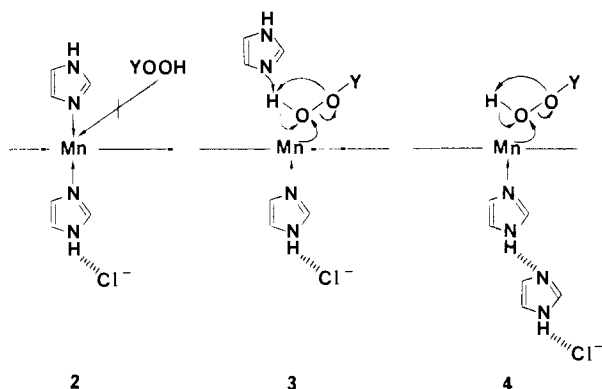
by Valentine et al.²⁰ who showed a stepwise coordination of (TPP)Fe^{III}(SbF₆) by imidazole and its derivatives in toluene. Investigations of the association constants of nitrogen and oxygen ligands to manganese(III) porphyrin species, though limited, indicate that the equilibrium constants for the formation of monoligated and bis-ligated species are comparable.²² In our hands, the monoimidazole and bisimidazole complexes of (TPP)Mn^{III} have similar absorption spectra and comparable formation constants. Walker¹⁶ has postulated that Cl⁻ hydrogen bonding to the imidazole moiety in TPP(Cl)Fe^{III}(ImH) (**1**) contributes to the association constant for ImH complexation. Inspection



of Table I shows that the β_2 for ImH complexation exceeds that for *N*-MeIm complexation by 10-fold. This may be due to hydrogen bonding as shown with **1**. Basicity and steric availability are the two factors which determine the ability of ligands to coordinate with metalloporphyrins. Steric hindrance to the complexation of (TPP)Mn^{III}Cl by 2,6-lutidine ($K_1 = 0.33$ M) is as expected.

Importance of Hydrogen Bonding in Determining the Rate Constants for Oxygen Transfer from YOOH to Imidazole-Ligated (TPP)Mn^{III}. Kinetic data for oxygen transfer from Ph₂C(CN)OOH and *t*-BuOOH to (TPP)Mn^{III} ligated with imidazole, *N*-methylimidazole, and 3,4-lutidine are summarized in Table III. According to eq 11, values of the rate constants k_2 and k_3 for oxygen transfer to monoligated and bis-ligated (TPP)Mn^{III}Cl were determined from the intercept and slope obtained from the linear relationship of $k_{\text{obsd}}/([(TPP)Mn^{III}Cl][N\text{-ligand}]_i)$ vs. $[N\text{-ligand}]_i$. Inspection of Table III shows that the k_2 values for all mono-*N*-ligated (TPP)Mn^{III}Cl complexes are similar. Oxygen transfer is seen to be immeasurably slow or nonexistent to the bis complexes when the nitrogen ligands are *N*-MeIm or 3,4-Py. (This finding explains the observation that epoxidation of olefins is inhibited by large excesses of pyridines.^{7c}) However, the rate constants (k_3) for oxygen donation from Ph₂C(CN)OOH and *t*-BuOOH to TPP(Cl)Mn^{III}(ImH)₂ were determined to be 552 and 1.3 M⁻¹ s⁻¹, respectively.

Structures **2**, **3**, and **4** are dynamically equivalent representations of the transition complex in the reaction of YOOH species with the bis imidazole complex of (TPP)Mn^{III}Cl. In **2**, the imidazoles



are bis-axial-ligated and there would appear to be no means for oxygen transfer to the fully ligated Mn(III). In **3**, a single imidazole serves as the ligand, while a second is in position to act

Table V. Values of k_{obsd} for Oxygen Transfer from Ph₂C(CN)OOH to Imidazole-Ligated (TPP)Mn^{III} in the Presence of 2,6-Lutidine^a

2,6-lutidine, M	k_{obsd} , s ⁻¹
1.43×10^{-3}	1.7×10^{-3}
2.86×10^{-3}	1.54×10^{-3}
5.72×10^{-3}	1.68×10^{-3}
8.58×10^{-3}	1.88×10^{-3}
1.14×10^{-2}	1.83×10^{-3}

^a The initial concentrations of the reaction mixture were as follows: [(TPP)Mn^{III}Cl] = 1.03×10^{-5} M, [ImH] = 3.95×10^{-3} M, [Ph₂C(CN)OOH] = 1.07×10^{-4} M, and [DPPH] = 3.95×10^{-3} M in CH₂Cl₂ at 25 °C.

as a general-base or spectator catalyst. Traylor and co-workers have presented evidence in support of general catalysis in oxygen transfer to iron(III) porphyrins from *t*-BuOOH and MCPBA.¹⁸ In structure **4**, the two imidazoles are hydrogen-bonded to form a single axial ligand. Imidazoles are known to exist in such hydrogen-bonded chains in aprotic solvents,¹⁶ and this type of ligation has been considered by Valentine.²⁰ Structure **2** certainly exists under our reaction conditions. However, since **2** and **3** are of the same composition, the concentration of **3** is given by $K^{3,2}[\mathbf{2}]$ and the two structures are kinetically equivalent. The choice



between structures **3** and **4** may be made on the basis that the nitrogen ligands *N*-MeIm and 3,4-Py can readily form the critical complex **3** but not **4**. The basicities of imidazole, *N*-methylimidazole, 3,4-lutidine, and 2,6-lutidine (Table I) are very close. If the observed k_3 values for the reaction of the YOOH species with TPP(Cl)Mn^{III}(ImH)₂ were due to the general-base catalysis of **3**, then the same general-base catalysis should be observed for (TPP)Mn^{III}(*N*-MeIm)₂Cl and (TPP)Mn^{III}(3,4-Py)₂Cl. Since there are no reactions of the bis-ligated (TPP)Mn^{III}Cl with the YOOH species when *N*-MeIm and 3,4-Py are ligands, the correct structure for (TPP)Mn^{III}(ImH)₂Cl must be **4**. Further evidence which supports the contention that the general-base mechanism is unimportant is provided by the data in Table V. 2,6-Lutidine is incapable of binding of manganese(III) tetraphenylporphyrin due to steric hindrance by the methyl substituents. It has a comparable basicity ($pK_a = 6.64$) to imidazole ($pK_a = 6.99$) and should, therefore, be comparable as a general base. Examination of Table V shows that 2,6-lutidine when added in excess has no influence on the rate of oxygen transfer from Ph₂C(CN)OOH to imidazole-ligated manganese TPP species.

It has been recognized in recent years that hydrogen bonding of the proximal ligands in peroxidase and cytochrome *c* plays a significant role in determining the structure and reactivity at the metal porphyrin center.²¹ Peroxidases are oxidized easier than the oxygen carriers, hemoglobin and myoglobin. It has been suggested that the stronger proximal hydrogen bonding in peroxidase results in a stronger Fe-N bond and a greater electron density on the iron, thus favoring the higher oxidation states. The influence of hydrogen bonding with simple metalloporphyrins has also been observed.^{23,24} Evidences in support of hydrogen bonding from coordinated N- and O-ligands with iron and manganese porphyrin complexes arises from EPR, ¹H NMR, optical spectra, and cyclic voltammetry.^{20,23,24} Here the reactive isomer of TPP(Cl)Mn^{III}(ImH)₂ was determined to be **4** with hydrogen bonding between two imidazoles. The difference in the kinetic results with imidazole and *N*-methylimidazole can be attributed to the capability of hydrogen bonding for the ligated imidazole but not for ligated *N*-methylimidazole. The latter is the most reactive of the nitrogen base ligated manganese(III) porphyrin species studied in the oxygen atom transfer from the YOOH species. The rate constants k_3 of Table IV may be compared to

(20) Quinn, R.; Nappa, M.; Valentine, J. S. *J. Am. Chem. Soc.* **1982**, *104*, 2588.

(21) (a) La Mar, G. N.; de Ropp, J. S. *J. Am. Chem. Soc.* **1982**, *104*, 5203. (b) Desbois, A.; Mazza, G.; Stetzkowski, F.; Lutz, M. *Biochim. Biophys. Acta* **1984**, *785*, 161. (c) Teraoka, J.; Kitagawa, T. *J. Biol. Chem.* **1981**, *256*, 3969. (d) Poulos, T. L.; Kraut, J. *J. Biol. Chem.* **1980**, *255*, 8199. (e) Brautigam, D. L.; Geinberg, B. M.; Margoliash, E.; Peisach, J.; Blumberg, W. E. *Ibid.* **1977**, *252*, 574.

(22) Kelly, S. L.; Kadish, K. M. *Inorg. Chem.* **1982**, *21*, 3631.

(23) Otsuka, T.; Ohya, T.; Sato, M. *Inorg. Chem.* **1985**, *24*, 776.

(24) (a) O'Brien, P.; Sweigart, D. A. *Inorg. Chem.* **1985**, *24*, 1405. (b) Tondreau, G. A.; Sweigart, D. A. *Ibid.* **1984**, *23*, 1060. (c) Doeff, M. M.; Sweigart, D. A. *Ibid.* **1982**, *21*, 3699.

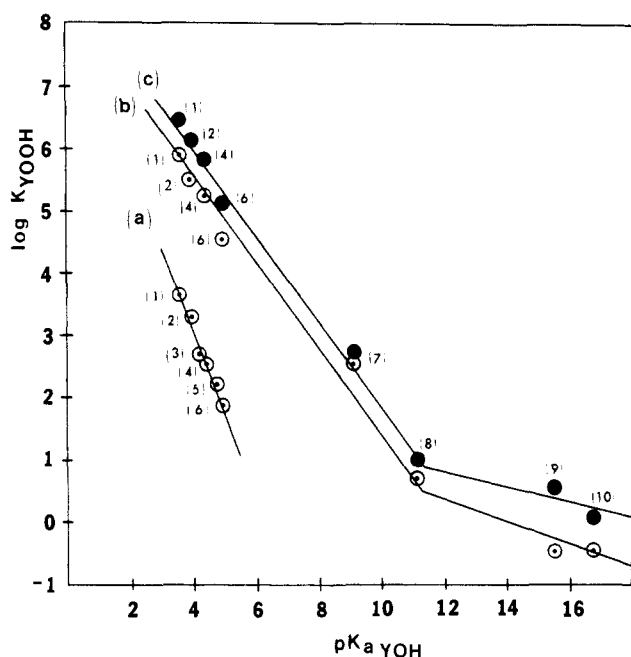


Figure 7. Plot of the log of the second-order rate constants for k_{YOOH} vs. the $\text{p}K_{\text{a}}$ of the carboxylic acid and alcohol leaving groups: (a) the reaction $(\text{TPP})\text{Mn}^{\text{III}}\text{Cl}$ with percarboxylic acids in benzonitrile (30 °C), (b) the reaction of $(\text{TPP}(\text{Cl})\text{Mn}^{\text{III}}\text{ImH})$ with percarboxylic acids and hydroperoxides, and (c) the reaction of $(\text{TPP}(\text{Cl})\text{Mn}^{\text{III}}(\text{ImH})_2)$ with percarboxylic acids and hydroperoxides (k_{YOOH}). (1) *p*-Nitroperbenzoic acid, (2) MCPBA, (3) 3-chloroperpropionic acid, (4) phenylperacetic acid, (5) 5-chloropervaleric acid, (6) perlauric acid, (7) diphenylhydroperoxyacetonitrile, (8) methyl diphenylhydroperoxyacetate, (9) cumyl hydroperoxide, and (10) *t*-BuOOH.

k_2 to appreciate this fact; however, the ratio k_3/k_2 represents a minimal which must be multiplied by the large but unknown constant $K^{4,2}$ to appreciate the kinetic advantage of the hydrogen-bonded structure 4.



The displacement of the manganese atom from the porphyrin plane is 0.265 Å in the complex $(\text{TPP})\text{Mn}^{\text{III}}\text{Cl}$.²⁵ However, when pyridine or methanol are coordinated as axial ligands as in the complexes of $(\text{TPP})\text{Mn}^{\text{III}}(\text{Py})\text{Cl}$ and $(\text{TPP})\text{Mn}^{\text{III}}(\text{CH}_3\text{OH})\text{N}_3$, the displacement is reduced to 0.12²⁶ and 0.085 Å,²⁷ respectively. Manganese(III) porphyrin imidazole and cyanide complexes²⁸ ($(\text{TPP})\text{Mn}^{\text{III}}(\text{ImH})_2$ and $(\text{TPP})\text{Mn}^{\text{III}}(\text{CN})_2$, respectively) have been identified as low spin. In an imidazolate-bridged polymer $[(\text{TPP})\text{Mn}^{\text{III}}(\text{Im})]_n$, the displacement of manganese to the porphyrin plane reflected an alteration of low and high spin.²⁹ Meunier^{7b} and Mansuy^{6d} have shown that pyridine and imidazole ligation of $(\text{TPP})\text{Mn}^{\text{III}}\text{Cl}$ results in an increase in the stereoselectivity of epoxidation of *cis*-stilbene (less *trans*-epoxide) when using NaOCl and cumyl hydroperoxides as oxygen-transfer agents. Therefore, it is clear that the stereoselectivity is increased with a manganese porphyrin coordinated by a stronger field ligand. From the present study, the rate constants for reaction of $(\text{TPP}(\text{Cl})\text{Mn}^{\text{III}}\text{ImH})$, $(\text{TPP}(\text{Cl})\text{Mn}^{\text{III}}(N\text{-MeIm}))$, and $(\text{TPP}(\text{Cl})\text{Mn}^{\text{III}}(3,4\text{-Py}))$ with YOOH are similar and much greater than for $(\text{TPP})\text{Mn}^{\text{III}}\text{Cl}$. The higher reactivity of 4, compared with the

monoimidazole complex, is assumed to be due to an increase in basicity of the ligated imidazole due to hydrogen-bonding with an accompanying increase in ease of oxidation of the manganese(III) moiety.

In Figure 7b, the $\log k_2$ values for the reaction of YOOH with $(\text{TPP}(\text{Cl})\text{Mn}^{\text{III}}\text{ImH})$ are plotted against the $\text{p}K_{\text{a}}$ for the corresponding leaving group (YOH). The slope of the linear free-energy plot in Figure 7b shows a break at a $\text{p}K_{\text{a}}$ for YOH of 11. This break is highly suggestive for a mechanism change at the $\text{p}K_{\text{a}}$ of YOH of ca. 11. GC analysis showed the yield of recovered ester $\text{PhCH}_2\text{CO}_2\text{CH}_3$ to be $91.6 \pm 1.7\%$ after the completion of the oxygen transfer from phenylperacetate (2.46×10^{-3} M) to $(\text{TPP})\text{Mn}^{\text{III}}\text{Cl}$ (2.81×10^{-3} M) in the presence of imidazole (4.5×10^{-3} M). Thus, the mechanism of oxygen transfer from a high monooxygen donation potential YOOH compound with a $\text{p}K_{\text{a}}$ smaller than 11 involves a heterolytic O–O bond cleavage. We assume the mechanism of oxygen transfer from a low monooxygen donation potential compound with a $\text{p}K_{\text{a}}$ larger than 11 involves rate-limiting homolytic O–O bond cleavage. The slopes of the linear free-energy plots were determined to be -0.72 for the heterolytic O–O bond scission and -0.19 for the homolytic O–O bond scission.

In Figure 7c, there is also plotted the log of the second-order rate constant (k_3) for the reaction of the YOOH species with $(\text{TPP})\text{Mn}^{\text{III}}(\text{ImH})_2\text{Cl}$ vs. the $\text{p}K_{\text{a}}$ of YOH. Again, a break at $\text{p}K_{\text{a}}$ of 11 is apparent. It may be assumed that the mechanisms for the reaction of YOOH with both $(\text{TPP}(\text{Cl})\text{Mn}^{\text{III}}\text{ImH})$ and $(\text{TPP})\text{Mn}^{\text{III}}(\text{ImH})_2\text{Cl}$ are similar. Therefore, heterolytic O–O bond cleavage occurs in oxygen transfer from all percarboxylic acids, diphenylhydroperoxyacetonitrile, and methyl diphenylhydroperoxyacetate, and a homolytic O–O bond cleavage occurs in the case when the $\text{p}K_{\text{a}}$ is > 11 for their corresponding leaving groups. The slopes in Figure 7c were determined to be -0.68 and -0.12 .

The mechanism change in Figure 7 at a $\text{p}K_{\text{a}}$ of 11 for the leaving group YOH is similar to the linear free-energy relation seen in the reaction of $(\text{TPP})\text{Fe}^{\text{III}}\text{Cl}$ and $(\text{TPP})\text{Co}^{\text{III}}\text{Cl}$ with YOOH compounds which show a break at $\text{p}K_{\text{a}}$ 9.^{17,30} As before, heterolytic O–O bond cleavage occurs in the case of oxygen transfer from high monooxygen donation potential compounds, which include percarboxylic acids and the most acidic alkyl hydroperoxides. Homolytic cleavage of an O–O bond is expected to be associated with little variation in k_{YOOH} with a change in the $\text{p}K_{\text{a}}$ of YOH as observed. The Brønsted (β_{lg}) values for $(\text{TPP}(\text{Cl})\text{Mn}^{\text{III}}\text{ImH})$ and $\text{Cl}\cdots\text{HIm}\cdots\text{HIm}\cdots(\text{TPP})\text{Mn}^{\text{III}}$ are very close to the $\beta_{\text{lg}} = -0.72$ ³⁰ obtained from the linear free-energy plot of the kinetic data for $(\text{TPP})\text{Co}^{\text{III}}\text{Cl}$ but much smaller than observed (-0.35) for the O–O bond heterolysis of YOOH observed with $(\text{TPP})\text{Cr}^{\text{III}}\text{Cl}$ and $(\text{TPP})\text{Fe}^{\text{III}}\text{Cl}$. Plot a in Figure 7 is from a previous study of oxygen transfer from percarboxylic acids to $(\text{TPP})\text{Mn}^{\text{III}}\text{Cl}$ in benzonitrile and is characterized by a β_{lg} value equal to -1.25 .⁵ The second-order rate constants, k_{YOOH} , for oxygen transfer from *p*-nitroperbenzoic acid to $(\text{TPP})\text{Mn}^{\text{III}}(\text{ImH})_2\text{Cl}$ and $(\text{TPP}(\text{Cl})\text{Mn}^{\text{III}}\text{ImH})$ compared with $(\text{TPP})\text{Mn}^{\text{III}}\text{Cl}$ in benzonitrile are 500- and 200-fold larger. Inspection of plots a, b, and c shows that imidazole ligation increases the rate constants for oxygen transfer from YOOH by about a factor of 100~1000. These rate constant increases must be expanded a bit to account for the change in solvent. In the reaction of $(\text{TPP})\text{Mn}^{\text{III}}\text{Cl}$ with MCPBA, the rate constants in benzonitrile was determined to be ~20-fold larger than the rate constant measured in methylene chloride. Therefore, the acceleration of the reaction in methylene chloride by an imidazole ligand may be taken to be about $10^3\text{--}10^4$.

Acknowledgment. This study has been supported by a grant from the National Institutes of Health.

Registry No. MCPBA, 937-14-4; ImH, 288-32-4; *N*-MeIm, 616-47-7; NAcPhIm, 24155-34-8; 3,4-Py, 583-58-4; 2,6-Py, 108-48-5; $(\text{TPP}(\text{Cl})$

(25) (a) Hoard, J. L. In "Porphyrins and Metalloporphyrins"; Smith, K. M., Ed.; Elsevier: Amsterdam, 1975; p 353. (b) Van Der Made, A. W.; Nolte, R. J. M. *J. Molec. Catal.* **1984**, *26*, 333.

(26) Kirner, J. F.; Scheidt, W. R. *Inorg. Chem.* **1975**, *14*, 2081.

(27) Day, V. W.; Stults, B. R.; Tasset, E. L.; Day, R. O.; Marianelli, R. S. *J. Am. Chem. Soc.* **1974**, *96*, 2650.

(28) Hansen, A. P.; Goff, H. M. *Inorg. Chem.* **1984**, *23*, 4519.

(29) Landrum, J. T.; Hatano, K.; Scheidt, W. R.; Reed, C. A. *J. Am. Chem. Soc.* **1980**, *102*, 6729.

(30) Lee, W. A.; Bruce, T. C. *Inorg. Chem.*, in press.

Mn^{III}ImH, 79969-69-0; (TPP)Mn^{III}(1mH)₂Cl, 100082-46-0; TPP(Cl)-Mn^{III}N-Melm, 79969-71-4; (TPP)Mn^{III}(N-Melm)₂Cl, 100082-48-2; TPP(Cl)Mn^{III}3,4-Py, 100082-47-1; (TPP)Mn^{III}(3,4-Py)₂Cl, 100082-49-3; TPP(Cl)Mn^{III}NAcPhIm, 100082-50-6; TPP(Cl)Mn^{III}2,6-Py, 100082-

51-7; (TPP)Mn^{III}Cl, 32195-55-4; Ph₂C(CN)OOH, 5233-67-0; (CH₃)₃-COOH, 75-91-2; *p*-NO₂-Ph-CO₂H, 943-39-5; PhCH₂CO₂H, 19910-09-9; CH₃(CH₂)₁₀CO₂H, 2388-12-7; Ph₂C(CO₂Me)OOH, 57272-44-3; PhC-(CH₃)₂OOH, 80-15-9.

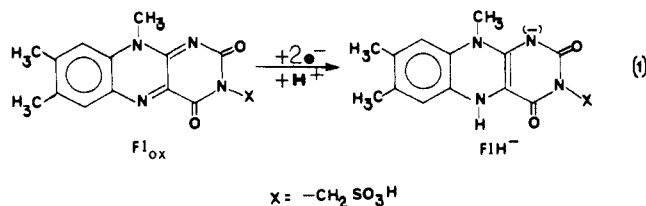
High- and Low-Potential Flavin Mimics. 3. 3,7,10-Trimethyl-(1*H*,3*H*,5*H*,7*H*,9*H*,10*H*)- pyrimido[5,4-*g*]pteridine-2,4,6,8-tetrone-Mediated Reduction of Carbon-Carbon Double Bonds α - β to an Acyl Function

Edward B. Skibo*[†] and Thomas C. Bruice*[‡]

Contribution from the Department of Chemistry, Arizona State University, Tempe, Arizona 85287, and the Department of Chemistry, University of California at Santa Barbara, Santa Barbara, California 93106. Received August 15, 1985

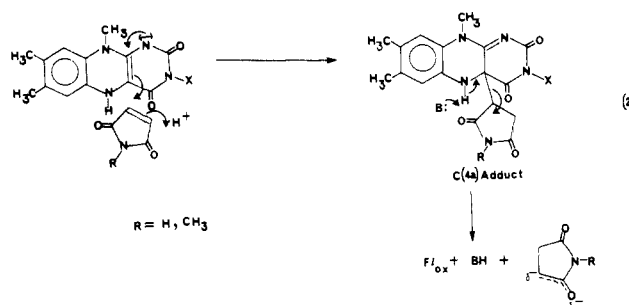
Abstract: The reduction of the carbon-carbon double bond of maleimide (MI), *N*-methylmaleimide (NMM), ethyl fumarate, diethyl fumarate, diethyl maleate, fumaric acid, and maleic acid was investigated by employing the low redox potential flavin mimic 3,7,10-trimethyl-(1*H*,3*H*,5*H*,7*H*,9*H*,10*H*)-pyrimido[5,4-*g*]pteridine-2,4,6,8-tetrone (PPTH₂) as the reductant. The reaction of these substrates with PPTH₂ to produce PPT_{ox} and the corresponding succinimide or succinate consists of three processes. The first process occurs on mixing and pertains to the formation of a mixture of N(1)- and C(4a)-substrate adducts of PPTH₂. The other two processes, which are kinetically distinguishable, pertain to the breakdown of each of these adducts to PPT_{ox} and the reduced substrate. Breakdown of the C(4a)-adduct is catalyzed by hydroxide and is independent of substrate concentration. Hydroxide catalysis is proposed to represent a concerted process whereby the hydroxide abstracts the N(5)-proton while the anionic reduced substrate is departing (Brønsted β approaching 1.0). Breakdown of the N(1)-adduct to the observed products is substrate-dependent pertaining to the rate-determining formation of the N(9),C(4a)-diadduct. In a fast step, base-catalyzed elimination from the C(4a)-position of the latter provides the reduced substrate anion and the N(9)-monosubstrate adduct of PPT_{ox}. Rapid dissociation of the N(9)-adduct then provides PPT_{ox}. It is concluded that the reduction of a carbon-carbon double bond to an acyl function by the low-potential flavin mimic proceeds via C(4a)-adducts. This conclusion and the principle of microreversibility infers that enzyme-bound flavins of high potential, as in dehydrogenating flavoenzymes, may oxidize succinates to fumarates via C(4a)-adducts.

Model studies have provided insights into the mechanisms of the diverse redox reactions mediated by flavoenzymes.¹ As a model for these reactions, the lumiflavin redox couple (Fl_{ox}/FlH⁻), or a suitable analogue thereof, is employed as an oxidant or reductant of the substrate in an enzyme-free reaction. Results



of such studies have served to provide a chemical basis upon which flavoenzyme mechanisms may rest. Flavoenzymes involved in oxidative formation and retroreduction of C-C double bonds α , β to a carbonyl group have been studied in this fashion. By employing FlH⁻ as the reductant for *N*-methylmaleimide (NMM) and maleimide (MI), Venkataram and Bruice² determined that electron transfer occurs via the C(4a)-adduct, eq 2.

It was concluded by these workers that succinic acid dehydrogenase and fumarate reductase³ may likewise transfer electrons via a similar adduct. The conclusion regarding succinic acid dehydrogenase invokes the principle of microreversibility which states that the transition state for the forward process (reduction of NMM and MI) is the same as that for the reverse process (oxidation of the corresponding succinimides). The



principle of microreversibility must be used in conjunction with the model approach since the redox potential of the enzyme-bound flavin is difficult to match with a mimic. Indeed the redox potentials of flavoenzymes may be far removed from that of the free cofactor in aqueous buffer (Fl_{ox}/FlH⁻, $E^{\circ\prime} = -0.189$ V). Notable examples are glucose oxidase⁴ (two-electron potential, $E^{\circ\prime} = 0.0$ V) and thiamine dehydrogenase⁵ (single-electron potentials of $E_1^{\circ\prime} = +0.08$ V and $E_2^{\circ\prime} = +0.03$ V). The reduction potential of

(1) (a) Bruice, T. C. *Acc. Chem. Res.* **1980**, *13*, 256. (b) Bruice, T. C. In "Biomimetic Chemistry"; Dolphin, D., McKenna, C., Murakami, Y., Tsuboshi, I., Eds.; Wiley: New York, 1980; ACS Adv. Chem. Ser. No. 191, p 89.

(2) Venkataram, U. V.; Bruice, T. C. *J. Am. Chem. Soc.* **1984**, *106*, 5703.

(3) Walsh, C. *Acc. Chem. Res.* **1980**, *13*, 148.

(4) Stankovich, M. T.; Schopfer, L. M.; Massey, V. *J. Biol. Chem.* **1978**, *253*, 4971.

(5) Edmondson, D. E.; Gomez-Moreno, C. In "Flavins and Flavoproteins"; Yagi, K., Yamano, T., Eds.; University Park Press: Baltimore, 1980; p 297.

[†] Arizona State University.

[‡] University of California at Santa Barbara.